Removal of heavy metallic ions from the aqueous solution using raw and modified coal ash

Vighnesh Prasad[a,b,*]

[a] Chemical Engineering, Indian Institute of Technology, Gandhinagar, Palaj, Gandhinagar, 382355, India

[b] Design and Project Engineering Department, CSIR – Institute of Minerals & Materials Technology, Bhubaneswar, Odisha, 751013, India

*Corresponding author: vprasad@immt.res.in, Tel. No.: +91 674 2379172

Abstract

The purpose of the present investigation is to explore the capability of Indian coal ash as a low-cost adsorbent for the adsorption of Cu^{2+}, Cd^{2+}, and Pb^{2+} metallic ions present in wastewater. It is observed that 5.14, 5.04 and 15.89% of Cu^{2+}, Cd^{2+}, and Pb^{2+} are removed using coal fly ash samples, which sharply increases to 99.8, 100 and 27.68%, when the same fly ash is treated with calcium. The removal of Cu^{2+}, Cd^{2+}, and Pb^{2+} ions increases from 41.3 - 99.9%, 79.1 - 100%, and 5.9 - 41%, respectively, when calcium-treated coal fly ash dosage varies from 1000-50000 ppm. These metallic ions adsorb on the silanol sites of raw coal ash. When treated coal ash is used, some metallic ions get precipitated as metal hydroxides, and the rest is adsorbed on calcium silicate hydrate in the form of metal silicate. Moreover, the metal removal rate also enhances from 0.99-5.14%, 1.31-5.04%, and 6.49-15.89% for Cu^{2+}, Cd^{2+}, and Pb^{2+} ions, respectively, when fine coal fly ash (d_{50} = 3.07 μm) is used instead of coarse bottom ash (d_{50} =

37.87 μm). The pseudo-first-order and pseudo-second-order kinetics models describe the experimental data reasonably well.

Keywords: Removal efficiency, Adsorption, Adsorbent, Precipitation, Heavy metals, Kinetics

1. INTRODUCTION

Electronic industries discharge a large amount of heavy and hazardous metals near water bodies, with copper (Cu^{2+}), lead (Pb^{2+}), and cadmium (Cd^{2+}) ions among the most common [1]. Besides, metal plating, mining, metallurgy, tanneries, and painting are also the source of these heavy metallic ions [2]. The elements with an atomic density of more than 6 g/cm^3 are referred to as heavy metals [3]. These are highly toxic because of their non-biodegradable and carcinogenic nature and severely contaminate the surface and groundwater sources [4,5]. Eco-friendly and safe disposal of wastewater containing these heavy metallic ions is a great concern for industrialists and environmentalists as low-cost alternatives to treat the wastewater are limited. The toxicological effects of Cu^{2+}, Cd^{2+}, and Pb^{2+} are diarrhea, salivation, nausea, vomiting, epigastric burning [6], cancer and organ system toxicity [7], oxidative stress, and neurological abnormalities [8], respectively. As per the World Health Organisation (WHO) and Environmental Protection Agency of the United States (USEPA), the maximum permissible limit of Cu^{2+}, Cd^{2+}, and Pb^{2+} in drinking water is 1.3, 0.005, and 0.015 ppm, respectively [9].

Ion exchange, adsorption, electrolytic, ultrafiltration, precipitation, solvent extraction, and reverse osmosis methods can remove metallic ions from wastewater [10–13]. However, the expensive methodology restricts their application in the commercial sectors [14]. Conversely, the adsorption is considered as one of the preferred methods as it is capable to remove even lower concentrations of heavy metals, demand less energy, and availability of a wide range of adsorbents [15]. The adsorption mechanism involves forming a layer of adsorbate on the surface of adsorbents. It is majorly classified as physisorption and chemisorption, where adsorbent and adsorbate attaches with weak vander waals attaractive forces and strong chemical forces, respectively. The adsorption on solid adsorbents mainly follows three steps: 1) Transit of metallic ions or pollutants from aqueous solution to the adsorbent surface, 2) adsorption on to the solid surface, and 3) movement within the adsorbent particle [16]. This process influences by various parameters including, pH, temperature, contact time, adsorbent dosage, adsorbent size, metal concentrations, volume treated, types of adsorption system, and co-existing ions [17].

The most commonly used activated carbon as an adsorbent due to its porous structure, larger surface area and chemical complexity, however it is expensive [1,2]. Similarly, the peculiar mechanical, chemical and physical properties of graphene makes it as greater adsorbent, however the bulk production at low cost limits its adoptability [18]. Thus, researchers have adopted some low-cost adsorbents, including lignin [19], clay [20], coal [21–23], biomass and biochar [24], zeolites [25], Azadirachta indica Leaves [26], geopolymer [27], nanocomposites [28], solid wastes [29–31], goethite [32], alumina [33], and chitosan [34]. However, the maximum metal removal efficiency with these adsorbents is still an area of research.

Some researchers have proposed raw fly ash as an adsorbent [4,35,36]. However, the low adsorption capacity of this coal by-product limits its broad applicability due to its small pore volume and crystalline structure [1,37]. Visa [38] reports that removal efficiency is less than 10% with raw coal ash adsorbent due to low surface area and heterogeneity charge on the surface. The adsorption of coal ash varies with the physical and chemical properties and status of the adsorption tests [11]. Bayat [5], and Soco and Kalembkiewicz [39] stipulate that the adsorption mechanism is mainly controlled by the silica and alumina present in the coal ash. The available data on the abatement of metallic ions using raw coal ash appears insufficient due to the limitation of test conditions. Besides, the metal removal capability of coal ash is not widely examined when metallic ions are present together in the aqueous solution. Investigators also used magnetic coating [40], acid and base treatment [41], thermochemical treatment [42], pelletization [2], and zeolitization [43] to improve the metal adsorption of fly ash. However, the information pertaining to enhancing the adsorption capacity and metal removal efficiency of coal ash is inadequate. Various surface modification methods to improve the metal removal rate of coal ash are tabulated in Table 1

The novelty of the present investigation includes 1) The use of two different sizes of coal by-product as adsorbents to investigate the effect of adsorbent sizes and, subsequently, the effect of specific surface area on the adsorbent capacity and metal removal efficiencies, which is rarely being found in the past works; 2) The role of calcium in the metal removal process has been sufficiently explained in this work. In contrast, previous works have yet to widely report this low-cost calcium treatment process; 3) The removal of multi-metallic ions (Cu^{2+}, Cd^{2+}, and Pb^{2+}) using a single dosage of low-cost adsorbent, which researchers have scarcely attempted in the past.

In the present study, coal ash is chosen as a test sample as it is readily available in large quantities at free of cost. Coal ash as an adsorbent solves mainly two issues: water quality improvement as adsorbent and waste utilization in coal-based thermal power plants. About 230 million tonnes of coal fly ash is generated in India annually, utilized in brick manufacturing, aggregates, road embankment, paint, cement manufacturing, and agriculture [55]. However, 100% utilization is still challenging for thermal power plants across the globe. This investigation aims to describe the role of particle size, contact time (t) between adsorbent and adsorbate, and calcium content on the adsorption capacity and removal efficiency of coal ash samples while handling a wastewater source containing Cu^{2+}, Cd^{2+} and Pb^{2+} ions.

2. Materials and method

2.1 Adsorbent and adsorbate

Two different particle sizes of coal ash were collected from Sabarmati Thermal Power Station, Gandhinagar, Gujarat, India. These powdered coal wastes were odorless and gray in color, and were used as received without further purification. The calcium carbonate ($CaCO_3$) - an odorless, white powder was procured from Sigma-Aldrich Chemicals Private Limited, Bangalore (Purity ≥ 99%) and further heated in a furnace (NaberthermLHT, GmBH) at 1200ºC to get calcium oxide (CaO) powder. A portion of the raw coal ash was mixed with CaO in the proportion of CaO/Coal ash=1/2 in a beaker containing 50 ml distilled water and stirred for 2 hrs. The latter mixture was kept in the oven for 24 hrs at 105ºC and grounded in powder form, termed calcium-treated coal ash (Ca-coal ash). The other portion of coal ash was used as received in the form of raw coal ash. Moreover, Copper (II) chloride, $CuCl_2$ (yellowish-brown, odorless, Purity ≥ 98, Hi-Media Laboratories Private Limited, Thane), Lead (II) nitrate, $Pb(NO_3)_2$ (Purity ≥ 99.5%, white and odorless, Finar chemical Ltd. Ahmedabad), and cadmium (II) nitrate, $Cd(NO_3)_2$ (Purity ≥ 99%, white and odorless, Finar chemical Ltd. Ahmedabad) were taken as adsorbates, which were used without further purification.

2.2 Equipment

The particle size distribution of the raw coal ash was determined with a particle size analyzer (CILAS – 1090). The morphology and qualitative elemental composition of the raw and Ca-coal ash samples were assessed with Field Emission Scanning Electron Microscope (FE-SEM) (JEOL-JSM7600F) and Energy Dispersive X-Ray Spectroscopy (EDS) (INCA Energy 250), respectively. The phase determinations of the raw and Ca-coal ash were analysed with X-Ray Powder Diffraction (XRD) (Xpert Pro, Malvern Panalytical) in the 2θ range of 5º - 90º. The concentration of three metallic ions Cu^{2+}, Cd^{2+} and Pb^{2+} in the aqueous solutions was determined using Induced coupled plasma-optical emission spectrometry (ICP-OES) (PerkinElmer, Avio 200). A standard pH meter (OAKTON, Eutech Instruments) was used to measure the pH of the aqueous solutions. The BET specific surface area of coal ash samples was determined using a surface area analyzer (Micromeritics ASAP 2020).

2.3 Adsorption studies

The adsorbents were dried at 105ºC for 24 hours to remove moisture. 50 ppm each of Cu^{2+}, Cd^{2+} and Pb^{2+} was added to 200 ml distilled water. The adsorption of metallic ions was studied after adding 10000 ppm of an adsorbent into the aqueous solution and continuously stirring it at 200 rpm in a bench shaker (DLAB, SK-O330-Pro). Aliquots were taken out at six different time intervals between 0-540 minutes and centrifuged at 10000 rpm for 5 minutes using SORVALL – ST8, Thermo Scientific. The centrifuged supernatant solutions were digested with 2% HNO_3 with a dilution factor of 25 to achieve the detection limit of ICP. The ICP spectrometry quantifies the concentration of Cu^{2+}, Cd^{2+}, and Pb^{2+} ions in the aqueous solution before and after the adsorption. The amount of metallic ions (in mg) adsorbed in one gram of coal ash is quantified as adsorption capacity, q_t (mg/g), expressed as Eq. (1) [1,56]. Moreover, the removal efficiency of coal ash is defined in terms of % removal of metallic ions from solution, given as Eq. (2) [1,56].

$$Adsorption\,capacity, q_t = (C_i - C_t)\frac{V}{m} \quad (1)$$

$$\%\,removal = \left(\frac{C_i - C_t}{C_i}\right) \times 100 \quad (2)$$

Here, C_i = Initial concentration of the metallic ions present in the aqueous solution (mg/L)

C_t = Concentration of the metallic ions in the aqueous solution at t minutes (mg/L)

V = Volume of the aqueous solution (L)

m = Mass of the adsorbent used in the aqueous solution (g)

3. Results and discussion

3.1 Characterization

The particle size distribution of raw coal ash samples is shown in Fig. 1. As evident, one of the coal ash samples, which has the largest particle size of 17 μm, with a median (d_{50}) = 3.07 μm, is known as coal fly ash (CFA). Moreover, the sample with the largest particle of 180 μm and d_{50} = 37.87 μm is categorized as coal bottom ash (CBA).

The SEM analysis indicates that the coal ash samples contain poly-dispersed solid spherical-shaped particles (Fig. 2a, c). Besides, a layer of calcium compound is observed on the surface of Ca-coal ash particles in the form of tinny rods (Fig. 2b, d).

The qualitative elemental composition of raw and Ca-coal ash is tabulated in Table 2. The analysis indicates that silica and alumina are the main components in raw coal ash; however, a small fraction of iron (Fe), potassium (K), calcium (Ca), and magnesium (Mg) is also present.

Similarly, the Ca-coal ash also contains all these elements with an increased calcium concentration.

The surface area data indicates that BET surface area drastically increases from 0.89 to 9.10 m^2/g when the CFA sample is treated with calcium (Ca-CFA). Similarly, the surface area improves from 0.53 to 8.84 m^2/g in the case of calcium treated CBA (Ca-CBA). The active sites for the interaction increase after treating the coal ash with calcium. As seen in the SEM images (Figs. 2b and 2d), tinny cylindrical rod structures on the coal ash surfaces can be observed. These structures facilitate additional surface areas $(A = 2\pi r(r+h))$, which vary with the height (h) and radius (r) of the rods. These statements agree with the work of Visa [38], who found an enhancement of surface area from 6.14-52.44 m^2/g and 1.013-37.3 m^2/g when coal fly ash underwent hydrothermal treatment with NaOH. Similarly, Zhao et al. [47] report that surface modification using the alkaline substance on coal ash makes the surface rough, which acts as a porous structure and increases the specific surface area.

Moreover, the XRD analysis indicates that the major mineral constituent is calcium silicate hydrate (CSH), while calcium silicate (CSI) and calcium hydroxide (CH) are also present in Ca-coal ash. In contrast, quartz (Q) and mullite (M) are the major components in the untreated raw coal ash sample (Fig. 3).

3.2 Effect of contact time (t) on the ion removal

The concentration of Cu^{2+}, Pb^{2+}, and Cd^{2+} ions in the aqueous solution with contact time (t) is presented in Fig. 4a, b, Fig. 5a, b, and Fig. 6a, b. As evident, C_t suddenly drops to a lower value and attains an equilibrium state in 10 minutes, especially for Cu^{2+} and Cd^{2+} ions. It indicates that these metallic ions do not adsorb appreciably on the coal ash surface after 10 minutes, suggesting the saturation of the coal ash particle surface.

The % removal of Cu^{2+} ions and q_t are noted to be 0.99% and 0.05 mg/g, and 5.14% and 0.26 mg/g at t = 30 minutes for raw CBA and CFA samples, respectively (Fig. 4c, d). It translates that CFA particles are ~ 5 times more efficient adsorbent than CBA. It is believed that a greater specific surface area of CFA facilitates more interaction with the metallic ions, promoting a higher % removal and q_t. Results agree with the studies of Ayala et al., [12], Sun et al. [57], and Maftouh et al. [15] who report that the finer grain size fraction facilitates larger specific surface area of functional groups leading to highest metal removal rate. Interestingly, the % removal and q_t are enhanced drastically when coal ash is treated with calcium. As shown in Fig. 4c, 5.14% of Cu^{2+} ions are removed from the solution in 30 minutes using raw CFA, which is increased to 99.8% when the same CFA is treated with calcium. Similarly, q_t is also enhanced from 0.26 – 5 mg/g when Ca-CFA is used (Fig. 4d). It qualitatively indicates that a thin layer of calcium on the coal ash surface makes the raw coal ash 20 times more efficient for removing Cu^{2+} ions.

Similar behaviour is observed during the removal of Pb^{2+} and Cd^{2+} ions from the solution using raw and Ca-coal ash, as shown in Figs. 5 and 6. The % removal of Pb^{2+} ions and q_t is around 6% and 0.3 mg/g for CBA particles, which increases to 16% and 0.8 mg/g, respectively, while using CFA as an adsorbent (Fig. 5c, d). Similarly, the % removal of Cd^{2+} ions and q_t are also increased from 1.3% and 0.07 mg/g to 5% and 0.25 mg/g, respectively, when CFA is used instead of CBA (Fig. 6c, d). Moreover, it is noted that around 16% of Pb^{2+} and 5% of Cd^{2+} ions are removed using raw CFA, which increases to 28% and 100%, respectively, when the same

CFA is treated with calcium (Fig. 5c and Fig. 6c). Also, q_t is enhanced from 0.8 – 1.4 mg/g, and 0.25 – 5 mg/g for Pb^{2+} and Cd^{2+} ions, respectively, when Ca-CFA is used (Fig. 5d and Fig. 6d).

3.3 Effect of adsorbent dosages on the ion removal

The effect of adsorbent concentration from 1000 - 50000 ppm on the % removal or metal removal efficiency of Ca-CFA has been studied for Cu^{2+}, Cd^{2+}, and Pb^{2+} metallic ions keeping a contact time of 30 minutes. The solution preparation and adsorption protocol were kept the same as mentioned in the section 2.

As evident in Fig. 7a, the q_t decreases with increase in CFA and Ca-CFA dosages, as the mass of the adsorbents (m) drastically increases with comparison to the loss of metallic ions $(C_i - C_t)$ in the solution (Eq.(1)). However, Ca-CFA exhibits higher q_t and metal removal efficiency as compared to CFA only (Fig.7). The Cu^{2+} ion removal is noted to be 1.7 – 19.9% when CFA dosages vary between 1000-50000 ppm. Interestingly, it increases to 41.3 - 99.9% when the exact dosage of Ca-CFA (1000-50000 ppm) is used. Similar trends are also observed in the case of Cd^{2+} and Pb^{2+} ions (Fig. 7b). These results also indicate that an excess amount of adsorbent dosages doesn't improve the metal removal rate appreciably.

3.4 Adsorption kinetics

The kinetics of the adsorption mechanism is modelled using the pseudo-first-order Lagergren equation (1^{st}) [58] and pseudo-second-order rate equation (2^{nd}) [59], expressed as Eqs. (3) and (4), respectively. These kinetics models predict the adsorption equilibrium and kinetic rate constants.

$$q_t = q_e\left(1\text{-}e^{-k_1 t}\right) \tag{3}$$

$$q_t = \frac{q_e^2 k_2 t}{\left(1+q_e k_2 t\right)} \tag{4}$$

Here, k_1 (h^{-1}) and k_2 (g/mg h) are the rate constants of pseudo-first-order and pseudo-second-order adsorptions, respectively. q_e (mg/g) is the amount of metallic ions adsorbed on coal ash at equilibrium. The kinetics models are fitted with the adsorption data of Cu^{2+}, Pb^{2+} and Cd^{2+}, as shown in Fig. 8, and kinetics parameters are tabulated in Table 3. A better regression coefficient (R^2) value implies that these models can well represent the experimental data of Cu^{2+} and Cd^{2+}.

The predictive adsorption capacity (q_{tk}) estimated using the kinetics models (Eqs. (3) and (4)) and experimental adsorption capacity (q_t) are illustrated for the CFA & Ca-CFA adsorbents, and Cu^{2+}, Cd^{2+}, and Pb^{2+} adsorbates. These values are tabulated in Tables 4 and 5. As evident in Table 4, the deviation in experimental adsorption with kinetics models is less than 10% for Ca-CFA adsorbent except Pb^{2+} ions. However, more than 10% deviation is found in the CFA adsorbent case (Table 5). It indicates that kinetics models poorly represent the adsorption results obtained using CFA adsorbent. In contrast, these models predict well when Ca-CFA is used as an adsorbent.

3.5 Removal mechanism of metallic ions from aqueous solution

Raw coal ash contains silica in abundant has a strong tendency to form chemical bonds with the metal ions [4,11]. The pH of the aqueous solution containing raw coal ash with Cu^{2+}, Pb^{2+}, and Cd^{2+} ions is 5, exhibiting the acidic nature of the suspension. The metal removal mechanism in the presence of raw coal ash is demonstrated in Fig. 9a. At low pH, the metallic ions can be removed by the adsorption process, where ions adsorb on the silica site of the coal ash surface, as expressed in Eq. (5) [10].

$$\text{-}SiO_2 + H_2O + Me^{2+} = \text{-}\,SiOMe^{+} + H_3O^{+} \qquad (5)$$

Here, Me represents the metallic ions.

The lower magnitudes of removal efficiency and q_t (Figs. 4, 5 and 6) in the presence of raw coal ash are due to the competition between H_3O^+ and cationic metal species (Cu^{2+}, Pb^{2+}, Cd^{2+}) [1,60]. Secondly, the oxygen atoms on the silica surface of coal ash react with water and form silanol (Si-OH), which gets positively ionized at low pH, resulting in the repulsion between the coal ash surface and these metal species [1]. Thus, the heavy metallic ions are not completely removed from the wastewater when only coal ash is used as an adsorbent, which demands further treatment (Fig. 9a).

It is observed that the aqueous solution becomes alkaline with pH = 11 when an equivalent amount of Ca-coal ash is substituted in place of raw coal ash. Here, the removal efficiency and q_t exhibit a higher value, as depicted in Figs. 4, 5 and 6. At higher pH, the silanol groups of coal ash dissociate and leave more anionic sites on the adsorbent surface, which becomes accessible to the metal species, leading to the formation of metallic silicate and metal hydroxides (Fig. 9b) [5,10,60]. Ayala et al. [12] also report that the metal cations hydrolyze and form metallic hydroxide precipitates at higher pH, as expressed by Eq. (6).

$$Me^{2+}(aq.) + nH_2O = Me\left(OH\right)_n^{2\text{-}n} + nH^{+} \qquad (6)$$

Cho et al., [61] report that the metal hydroxyl complexes have a higher affinity than the completely hydrated metals to adsorb on the adsorbent surface since the -OH group of the metal reduces the free energy requirement for adsorption.

Besides, Ca-coal ash also promotes the formation of calcium silicate hydrate (CSH) (Fig. 3), which acts as an excellent binding agent to heavy metallic ions [37,60], leading to the formation of calcium metallic silicate compound, as expressed in Eq. (7) [5].

$$nCaSiO_3HSiO_3^- + Me\left(OH\right)_2 \Leftrightarrow nCaSiO_3MeSiO_3 + H_2O + OH^- \qquad (7)$$

Here, removing metallic ions from the aqueous suspension is driven by adsorption and precipitation mechanisms when Ca-coal ash is used as an adsorbent (Fig. 9b). In contrast, when raw coal is used, metallic ions are removed purely by the adsorption process (Fig. 9a).

After the adsorption tests, the settled mass upon centrifugation is dried and further analyzed through SEM and EDS. As shown in Fig. 10b, d, the compounds of calcium metallic silicate and metallic hydroxide precipitates can be observed on the surface of Ca-CFA at *t* = 30 minutes, which is qualitatively supported by EDS analysis (Table 6). The higher concentration of metallic elements in Ca-CFA suggests its higher metal removal efficiency and q_t (Table 6).

The same centrifuged solids of raw and Ca-CFA are further assessed with XRD to quantify the constituents present in samples after the adsorption tests. XRD confirms the formation of metal hydroxides and compounds of calcium metallic silicate with a small fraction of metal oxides in Ca-CFA (Fig. 11). These results also suggest that a portion of metallic ions is removed as hydroxide precipitates, and the rest are removed as calcium silicate compounds. On the other hand, the raw CFA contains metallic silica complexes, indicating the adsorption of heavy ions on the silica surface. Other elements like quartz and metal oxides are also present in the raw CFA.

3.6 Contribution of calcium on the removal of metallic ions

In this set of experiments, only CaO and Ca-CFA are being used as adsorbents. Precautions have been taken to ensure that both the adsorbents contain an equal amount of CaO. The pH of the aqueous ionic solutions in both adsorbents is maintained at ~ 11 using sulphuric acid and sodium hydroxide.

The concentration of metallic ions in the solution drastically decreases with *t* and reaches equilibrium within 10 minutes, as presented in Fig. 12a, c, and e. The % removal of Cu^{2+}, Pb^{2+}, and Cd^{2+} ions in the presence of CaO are noted to be 79, 19, and 99%, respectively, at $t = 30$ minutes. However, it is increased to 99.8, 28, and 100%, respectively, when the same amount of CaO is added to CFA (Fig. 12b, d, and f). It is found that CaO in the ionic solution increases the pH, promoting the formation of metal hydroxides; consequently, the metallic ions are removed through precipitation only. On the other hand, the combination of CaO and coal ash leads to the formation of calcium silicate hydrate (CSH) and hydroxides, which remove the metallic ions through adsorption and precipitation. Moreover, CaO as an adsorbent appears to be expensive. However, a thin layer of calcium on coal ash makes it an efficient and low-cost adsorbent, supporting the 100% utilization of the coal by-products. The ions-loaded coal ash samples are proposed to be disposed of in the empty mines as mine backfilling material. In this way, it can address the problem of mine subsidence, environment-friendly disposal of hazardous metallic elements, and utilization of coal by-products.

4 Conclusion:

The present investigation demonstrates that the removal efficiency and adsorption capacity *(q_t)* of raw coal ash are enhanced after treating it with calcium. The % removal of Cu^{2+}, Pb^{2+} and Cd^{2+} and q_t of coal ash increases with the contact time *(t)* and adsorbent dosages. It achieves an equilibrium state in 10 minutes, after which no significant metal removal occurs. Due to the larger surface area, the removal efficiency and q_t of fine CFA are higher than coarser CBA. The metallic ions are removed by the adsorption of ions to the silica sites of the raw coal ash. Interestingly, the calcium compound on the coal ash surface raises the pH of the ionic solution, and forms calcium silicate hydrate, which accelerates the metal removal rate through adsorption and precipitation. The adsorption kinetics well describes the experimental data of the adsorption tests. Results indicate that the removal efficiency and q_t of various adsorbents are in the order of Ca-CFA>Ca-CBA>CFA>CBA. In addition, the removal of metallic ions from the wastewater solution is in the order of $Cd^{2+} > Cu^{2+} > Pb^{2+}$.

Acknowledgment

The author thanks the characterization division of IIT Gandhinagar and CSIR – IMMT Bhubaneswar for providing the characterization facilities. The author is also thankful to Dr. Superb Misra, IIT Gandhinagar, for granting his consent to publish this work. The author appreciates the valuable discussions with Dr. Prateek Goyal and Dr. Nilabh Dish during this study. The author also thanks the Director, CSIR - IMMT Bhubaneswar, for the permission to write/edit this draft.

Declaration of competing interest

The author has no competing interests to declare.

References

[1] He, K., Chen, Y., Tang, Z. et al. "Removal of heavy metal ions from aqueous solution by zeolite synthesized from fly ash", *Environmental Science and Pollution Research*, **23**, pp.2778-2788 (2016).

[2] Papandreou, A., Stournaras, C.J., and Panias, D. "Copper and cadmium adsorption on pellets made from fired coal fly ash", *Journal of Hazardous Materials*, **148**(3), pp.538-547 (2007).

[3] Xiyili, H., Çetintaş, S., and Bingöl, D. "Removal of some heavy metals onto mechanically activated fly ash: Modeling approach for optimization, isotherms, kinetics and thermodynamics", *Process Safety and Environmental Protection*, **109**, pp.288-300 (2017).

[4] Wang, S. and Wu, H. "Environmental-benign utilisation of fly ash as low-cost adsorbents", *Journal of hazardous materials*, **136**(3), pp.482-501(2006).

[5] Bayat, B. "Comparative study of adsorption properties of Turkish fly ashes: I. The case of nickel (II), copper (II) and zinc (II)", *Journal of hazardous materials*, **95**(3), pp.251-273 (2002).

[6] Fewtrell, L., Kay, D., Jones, F., et al. "Copper in drinking water—an investigation into possible health effects", *Public Health*, **110**(3), pp.175-177 (1996).

[7] Rahimzadeh, M.R., Rahimzadeh, M.R., Kazemi, S., et al. "Cadmium toxicity and treatment: An update", *Caspian journal of internal medicine*, **8**(3), p.135 (2017).

[8] Ara, A., and Usmani, J.A. "Lead toxicity: a review", *Interdisciplinary toxicology*, **8**(2), p.55 (2015).

[9] Aigbe, U. O., Ukhurebor, K. E., Onyancha, R. B., et al. "Fly ash-based adsorbent for adsorption of heavy metals and dyes from aqueous solution: a review", *Journal of Materials Research and Technology*, **14**, pp.2751-2774 (2021).

[10] Ricou-Hoeffer, P., Lecuyer, I., and Le Cloirec, P. "Experimental design methodology applied to adsorption of metallic ions onto fly ash", *Water Research*, **35**(4), pp.965-976 (2001).

[11] Lin, C.J., and Chang, J.E. "Effect of fly ash characteristics on the removal of Cu (II) from aqueous solution", *Chemosphere*, **44**(5), pp.1185-1192 (2001).

[12] Ayala, J., Blanco, F., Garcìa, P., et al. "Asturian fly ash as a heavy metals removal material", *Fuel*, **77**(11), pp.1147-1154 (1998).

[13] Balsamo, M., Di Natale, F., Erto, A., et al. "Arsenate removal from synthetic wastewater by adsorption onto fly ash", *Desalination*, **263**(1-3), pp.58-63 (2010).

[14] Qasem, N.A., Mohammed, R.H., and Lawal, D.U. "Removal of heavy metal ions from wastewater: A comprehensive and critical review", *Npj Clean Water*, **4**(1), p.36 (2021).

[15] Maftouh, A., El Fatni, O., El Hajjaji, S., et al. "Comparative review of different adsorption techniques used in heavy metals removal in water", *Biointerface Research in Applied Chemistry*, **13**, p.397 (2023).

[16] Raji, Z., Karim, A., Karam, A., et al. "Adsorption of heavy metals: Mechanisms, kinetics, and applications of various adsorbents in wastewater remediation—A review", *Waste*, **1**(3) pp. 775-805 (2023).

[17] Aigbe, U. O., Ukhurebor, K. E., Onyancha, R. B., et al. "Fly ash-based adsorbent for adsorption of heavy metals and dyes from aqueous solution: a review", *Journal of Materials Research and Technology*, **14**, pp.2751-2774 (2021).

[18] Kong, Q., Shi, X., Ma, W., et al. "Strategies to improve the adsorption properties of graphene-based adsorbent towards heavy metal ions and their compound pollutants: A review", *Journal of Hazardous Materials*, **415**, pp.125690 (2021).

[19] Srivastava, S.K., Singh, A.K., and Sharma, A. "Studies on the uptake of lead and zinc by lignin obtained from black liquor–a paper industry waste material", *Environmental technology*, **15**(4), pp.353-361 (1994).

[20] Hizal, J. and Apak, R. "Modeling of cadmium (II) adsorption on kaolinite-based clays in the absence and presence of humic acid", *Applied Clay Science*, **32**(3-4), pp.232-244 (2006).

[21] Xu, H., Wang, Y., Huagn, G., et al. "Removal of quinoline from aqueous solutions by lignite, coking coal and anthracite. Adsorption kinetics", *Physicochemical Problems of Mineral Processing*, **52**(1), pp.397-408 (2016).

[22] Xu, H., Sun, X., Yu, Y., et al. "Removal of quinoline using various particle sizes anthracite: adsorption kinetics and adsorption isotherms", *Physicochemical Problems of Mineral Processing*, **55**(1), pp.196-207 (2019).

[23] Xu, H., Wang, P., Ning, K., et al. "Effect of different acid-modified coking coals on quinoline adsorption", *ACS omega*, **4**(24), pp.20503-20508 (2019).

[24] Sireesha, S., Agarwal, A., Sopanrao, K.S., et al. "Modified coal fly ash as a low-cost, efficient, green, and stable adsorbent for heavy metal removal from aqueous solution", *Biomass Conversion and Biorefinery*, pp.1-24 (2022).

[25] Panek, R., Medykowska, M., Wiśniewska, M., et al. "Simultaneous removal of Pb2+ and Zn2+ heavy metals using fly ash Na-X zeolite and its carbon Na-X (C) composite", *Materials*, **14**(11), p.2832.(2021)

[26] Elkhaleefa, A., Ali, I.H., Brima, E.I., et al. "Evaluation of the adsorption efficiency on the removal of lead (II) ions from aqueous solutions using Azadirachta indica leaves as an adsorbent", *Processes*, **9**(3), p.559 (2021).

[27] Mužek, M.N., Svilović, S., and Zelić, J. "Fly ash-based geopolymeric adsorbent for copper ion removal from wastewater", *Desalination and Water Treatment*, **52**(13-15), pp.2519-2526 (2014).

[28] Zhao, G., Huang, X., Tang, Z., et al. "Polymer-based nanocomposites for heavy metal ions removal from aqueous solution: a review", *Polymer Chemistry*, **9**(26), pp.3562-3582 (2018).

[29] Nowak, B., Aschenbrenner, P., and Winter, F. "Heavy metal removal from sewage sludge ash and municipal solid waste fly ash—a comparison", *Fuel processing technology,* **105**, pp.195-201 (2013).

[30] Renu, M.A., Singh, K., Upadhyaya, S., et al. "Removal of heavy metals from wastewater

using modified agricultural adsorbents" *Materials Today: Proceedings*, **4**(9), pp.10534-10538 (2017).

[31] Fu, F. and Wang, Q. "Removal of heavy metal ions from wastewaters: a review", *Journal of environmental management*, **92**(3), pp.407-418 (2011).

[32] Saito, T., Koopal, L.K., Nagasaki, S., et al. "Analysis of copper binding in the ternary system Cu2+/humic acid/goethite at neutral to acidic pH", *Environmental science & technology*, **39**(13), pp.4886-4893 (2005).

[33] Wu, C.H., Lin, C.F., Ma, H.W., et al. "Effect of fulvic acid on the sorption of Cu and Pb onto γ-Al2O3", *Water research*, **37**(4), pp.743-752 (2003).

[34] Yan, W.L. and Bai, R. "Adsorption of lead and humic acid on chitosan hydrogel beads", *Water Research*, **39**(4), pp.688-698 (2005).

[35] Moyo, M., Muguni, L., and Nyamunda, B.C. "Optimisation of copper and zinc ions removal from aqueous solution by coal fly ash as an adsorbent", *International Journal of Engineering Science & Technology*, **4**, pp.1760–1766 (2012).

[36] Musapatika, E. T., Onyango, M. S., and Aoyi, O. "Cobalt (II) removal from synthetic wastewater by adsorption on South African coal fly ash", *South African Journal of Science*, **106**(9), pp.1-7 (2010).

[37] Ahmaruzzaman, M. "A review on the utilization of fly ash", *Progress in energy and combustion science*, **36**(3), pp.327-363 (2010).

[38] Visa, M. "Synthesis and characterization of new zeolite materials obtained from fly ash for heavy metals removal in advanced wastewater treatment", *Powder Technology*, **294**,

pp.338-347 (2016).

[39] Sočo, E. and Kalembkiewicz, J. "Adsorption of nickel (II) and copper (II) ions from aqueous solution by coal fly ash", *Journal of Environmental Chemical Engineering*, **1**(3), pp.581-588 (2013).

[40] Pengthamkeerati, P., Satapanajaru, T., Chatsatapattayakul, N., et al. "Alkaline treatment of biomass fly ash for reactive dye removal from aqueous solution" *Desalination*, **261**(1-2), pp.34-40 (2010).

[41] Hussain, Z., Chang, N., Sun, J., et al. "Modification of coal fly ash and its use as low-cost adsorbent for the removal of directive, acid and reactive dyes", *Journal of Hazardous Materials*, **422**, p.126778 (2022).

[42] Eteba, A., Bassyouni, M., and Saleh, M., "Utilization of chemically modified coal fly ash as cost-effective adsorbent for removal of hazardous organic wastes", *International Journal of Environmental Science and Technology*, **20**(7), pp.7589-7602 (2023).

[43] Kobayashi, Y., Ogata, F., Saenjum, C., et al. "Adsorption/desorption capability of potassium-type zeolite prepared from coal fly ash for removing of Hg2+", *Sustainability*, **13**(8), p.4269 (2021).

[44] Darmayanti, L., Notodarmodjo, S., and Damanhuri, E. "Removal of Copper (II) Ions in Aqueous Solutions by Sorption onto Fly Ash", *Journal of Engineering & Technological Sciences*, **49**(4) (2017).

[45] Al-Harahsheh, M. S., Al Zboon, K., Al-Makhadmeh, L., et al. "Fly ash based geopolymer for heavy metal removal: A case study on copper removal", *Journal of Environmental*

Chemical Engineering, **3**(3), pp.1669-1677 (2015).

[46] Ankrah, A. F., Tokay, B., and Snape, C. E. "Heavy metal removal from aqueous solutions using fly-ash derived zeolite NaP1", *International Journal of Environmental Research*, **16**(2), pp.17 (2022).

[47] Zhao, X., Zhao, H., Huang, X., et al. "Effect and mechanisms of synthesis conditions on the cadmium adsorption capacity of modified fly ash" *Ecotoxicology and Environmental Safety*, **223**, pp.112550 (2021).

[48] Vu, D. H., Bui, H. B., Bui, X. N., et al. "A novel approach in adsorption of heavy metal ions from aqueous solution using synthesized MCM-41 from coal bottom ash", *International Journal of Environmental Analytical Chemistry*, **100**(11), pp.1226-1244 (2020).

[49] Joseph, I. V., Tosheva, L., and Doyle, A. M. "Simultaneous removal of Cd (II), Co (II), Cu (II), Pb (II), and Zn (II) ions from aqueous solutions via adsorption on FAU-type zeolites prepared from coal fly ash", *Journal of Environmental Chemical Engineering*, **8**(4), 103895 (2020).

[50] Singh, N. B., Agarwal, A., De, A., et al. "Coal fly ash: an emerging material for water remediation" *International Journal of Coal Science & Technology*, **9**(1), pp.44 (2022).

[51] Zhang, J., Yan, M., Sun, G., et al. "Simultaneous removal of Cu (II), Cd (II), Cr (VI), and rhodamine B in wastewater using TiO2 nanofibers membrane loaded on porous fly ash ceramic support", *Separation and Purification Technology*, **272**, pp.118888 (2021).

[52] Buema, G., Harja, M., Lupu, N., et al. "Adsorption performance of modified fly ash for

copper ion removal from aqueous solution", *Water*, **13**(2), pp.207 (2021).

[53] Segneanu, A. E., Marin, C. N., Vlase, G., et al. "Highly efficient engineered waste eggshell-fly ash for cadmium removal from aqueous solution", *Scientific Reports*, **12**(1), pp.9676 (2022).

[54] Harja, M., Buema, G., Lupu, N., et al. "Fly ash coated with magnetic materials: Improved adsorbent for Cu (II) removal from wastewater", *Materials*, **14**(1), p.63 (2020).

[55] Boro, J. R. "Report on fly ash generation at coal / lignite based thermal power stations and its utilization in the country for the year 2020-21", *Central Electricity Authority, New Delhi* (2021)

[56] Xu, H., Qin, Q., Zhang, C., et al. "Adsorption of organic constituents from reverse osmosis concentrate in coal chemical industry by coking coal", *Processes*, **7**(1), pp.44 (2019).

[57] Sun, X., Ma, L., Ye, G., et al. "Phenol adsorption kinetics and isotherms on coal: effect of particle size", *Energy Sources, Part A: Recovery, Utilization, and Environmental Effects*, **43**(4), pp.461-474 (2021).

[58] Ho, Y.S. and Chiang, C.C. "Sorption studies of acid dye by mixed sorbents" *Adsorption*, **7**, pp.139-147 (2001).

[59] Ho, Y.S. and McKay, G. "Pseudo-second order model for sorption processes", *Process biochemistry*, **34**(5), pp.451-465 (1999).

[60] Ricou, P., Lecuyer, I., and Le Cloirec, P. "Removal of Cu2+, Zn2+ and Pb2+ by adsorption onto fly ash and fly ash/lime mixing", *Water Science and Technology*, **39**(10-

11), pp.239-247 (1999).

[61] Cho, H., Oh, D., and Kim, K. "A study on removal characteristics of heavy metals from aqueous solution by fly ash", *Journal of hazardous materials*, **127**(1-3), pp.187-195. (2005)

List of Table captions

List of Figure captions

Fig. 1 Particle size distribution of raw coal ash samples

Fig. 2 SEM images of Raw coal ash (a) 3000x (c) 50000x; and Calcium-treated coal ash (b) 3000x (d) 50000x

Fig. 3 XRD analysis of raw coal ash and calcium-treated coal ash (Ca-coal ash)

Fig. 4 Adsorption of Cu^{2+} on raw and calcium-treated coal ash (Ca-CFA: Calcium-treated coal fly ash, CFA: Coal fly ash, Ca-CBA: Calcium-treated coal bottom ash, CBA: Coal bottom ash)

Fig. 5 Adsorption of Pb^{2+} on raw and calcium-treated coal ash (Ca-CFA: Calcium-treated coal fly ash, CFA: Coal fly ash, Ca-CBA: Calcium-treated coal bottom ash, CBA: Coal bottom ash)

Fig. 6 Adsorption of Cd^{2+} on raw and calcium-treated coal ash (Ca-CFA: Calcium-treated coal fly ash, CFA: Coal fly ash, Ca-CBA: Calcium-treated coal bottom ash, CBA: Coal bottom ash)

Fig. 7 (a) Adsorption (b) removal efficiency of CFA and Ca-CFA adsorbents varying from 1000-50000 ppm (CFA: Coal fly ash, Ca-CFA: Calcium-treated coal fly ash)

Fig. 8 Adsorption kinetics of Cu^{2+}, Pb^{2+} and Cd^{2+} ions on raw coal ash and calcium-treated coal ash (Ca-CFA: Calcium-treated coal fly ash, CFA: Coal fly ash, Ca-CBA: Calcium-treated coal bottom ash, CBA: Coal bottom ash)

Fig. 9 Metal removal mechanism (a) raw coal ash (b) calcium-treated coal ash (Ca-coal ash)

Fig. 10 SEM images of raw CFA (a) 10000x (c) 20000x; and Ca-CFA (b) 10000x (d) 20000x at t = 30 minutes (CFA: coal fly ash, Ca-CFA: calcium-treated coal fly ash)

Fig. 11 XRD analysis of raw CFA and Ca-CFA at t = 30 minutes (CFA: coal fly ash, Ca-CFA: calcium-treated coal fly ash, a: Cadmium silicate, b: calcium silicate, c: cadmium hydroxide, d: compound of copper and cadmium, e: Cadmium oxide, g: lead silicate, h: lead hydroxide, i: lead aluminum oxide, j: lead oxide, m: mullite, n: calcium copper silicate, q: quartz, o: copper hydroxide, p: copper oxide)

Fig. 12 Adsorption of Cu^{2+}, $Pb^{2+}$and Cd^{2+} ions on CaO and Ca-CFA (CaO: calcium oxide, Ca-CFA: calcium-treated coal fly ash)

List of Tables

Table 1 Comparison of removal efficiencies of coal ash treated with various methods

Surface modification	**Adsorbate**	**Conditions**	**Removal efficiency (%)**	**References**
NaOH-treated fly ash 1	Cu^{2+}	t = 180 minutes	90%	[44]
		Adsorbent = 10g/L		
NaOH- treated fly ash 2	Cu^{2+}	C_i = 100 ppm	50%	
HNO_3-treated fly ash	Cd^{2+}	t = 240 minutes	5%	[1]
	Cu^{2+}	Adsorbent = 5g/L	8%	
	Pb^{2+}	C_i = 100 ppm	40%	
Hydrothermal treated fly ash	Cd^{2+}	t = 30 minutes	52%	[38]
	Cu^{2+}	Adsorbent = 4g/L	43%	
	Pb^{2+}	$C_{i,Cd}$ = 600 ppm	66%	
		$C_{i,Cu}$ = 250 ppm		
		$C_{i,pb}$ = 1000 ppm		
Fly ash based geopolymer	Cu^{2+}	t = 120 minutes	90%	[45]
		Adsorbent = 2g/L		
		C_i = 100 ppm		
Fly ash based zeolite	Cu^{2+}	t = 30 minutes	23%	[46]
	Pb^{2+}	Adsorbent = 1g/L	96%	

		$C_{i,Cu}$ = 150 ppm		
		$C_{i,Pb}$ = 100 ppm		
NaOH-treated fly ash	Cd^{2+}	t = 30 minutes	73%	[47]
		Adsorbent = 1g/L		
		C_i = 100 ppm		
NaOH-treated fly ash (synthesis)	Cd^{2+}	t = 24 hours	43.98%	[48]
	Cu^{2+}	Adsorbent = 1.67 g/L	41.66%	
	Pb^{2+}	C_i = 100 ppm	99.4%	
Hydrothermal-treated fly ash	Cd^{2+}	t = 30 minutes	88%	[49]
	Cu^{2+}	C_i = 200 ppm	92%	
Boric acid-treated fly ash	Cu^{2+}	t = 30 minutes	60%	[12]
		C_i = 280 ppm		
NaOH-treated fly ash	Pb^{2+}	t = 30 minutes	50%	[50]
		Adsorbent = 120g/L		
TiO_2-treated fly ash	Cd^{2+}	t = 30 minutes	18%	[51]
	Cu^{2+}	Adsorbent = 10g/L	66%	
		C_i = 100 ppm		
Fly-ash based Zeolite	Cu^{2+}	t = 12 hours	99%	[24]
		Adsorbent = 25g/L		
NaOH-treated fly ash	Cu^{2+}	t = 30 minutes	60%	[52]

		Adsorbent = 10g/L C_i = 300 ppm		
Eggshell coated fly ash	Cd^{2+}	t = 30 minutes Adsorbent = 5g/L C_i = 28.5 ppm	20%	[53]
Magnetite coated fly ash	Cu^{2+}	t = 1440 minutes Adsorbent = 10g/L C_i = 150 ppm	60%	[54]
CaO-treated coal fly ash	Cd^{2+} Cu^{2+} Pb^{2+}	t = 30 minutes C_i = 150 ppm Adsorbent = 10g/L	100% 99.8% 28%	This work

t = contact time (minutes), C_i = Initial concentration of metallic ions (mg/L), Calcium oxide (CaO), Sodium hydroxide (NaOH), Titanium dioxide (TiO_2), Nitric acid (HNO_3)

Table 2 Qualitative elemental composition of raw coal ash and Ca-coal ash

Elements	Weight%	
	Raw coal ash	Ca-Coal ash
O	50.16	43.86
Al	16.05	15.95
Si	30.11	29.27

K	0.43	0.38
Ca	0.99	8.52
Fe	1.90	1.72
Mg	0.36	0.30

Ca-coal ash: Calcium-treated coal ash

Table 3 Kinetic parameters of heavy metallic ions adsorption on raw coal ash and Ca-coal ash

Adsorbate	Adsorbent	First-order kinetics			Second-order kinetics		
		q_e (mg/g)	k_1 (h^{-1})	R^2	q_e (mg/g)	k_2 (g/mg h)	R^2
Cu^{2+}	Ca-CFA	4.94	90.66	0.99	4.94	1.86E43	0.99
	CFA	0.23	185.50	0.96	0.24	1.062	0.97
	Ca-CBA	4.90	75.56	0.99	4.90	2.13E20	0.99
	CBA	0.15	163.70	0.97	0.17	0.800	0.98
Pb^{2+}	Ca-CFA	1.47	4.32E45	0.94	1.47	769.1	0.94
	CFA	0.74	3.34E45	0.90	0.80	0.101	0.94
	Ca-CBA	0.72	5.04E44	0.83	0.79	0.098	0.80
	CBA	0.48	2.24E44	0.80	0.48	370.2	0.80
	Ca-CFA	5.00	12.82	0.99	5.00	3.72E11	0.99

	CFA	0.14	153.60	0.96	0.13	4.87	0.99
Cd^{2+}	Ca-CBA	5.00	12.83	0.99	5.00	1.61E12	0.99
	CBA	0.08	84.38	0.97	0.08	4.84	0.99

Ca-coal ash: Calcium-treated coal ash, Ca-CFA: Calcium-treated coal fly ash, CFA: Coal fly ash, Ca-CBA: Calcium-treated coal bottom ash, CBA: Coal bottom ash

Table 4 Adsorption capacities from experiments and kinetic models for Ca-CFA adsorbent

Adsorbate	Adsorption capacity, mg/g		Contact time *(t)*, Minutes				
			10	30	60	240	540
Cu^{2+}	q_{tk}	1st	4.939	4.94	4.94	4.94	4.94
		2nd	4.94	4.94	4.94	4.94	4.94
	q_t		4.965	4.9715	4.945	4.9	4.905
Pb^{2+}	q_{tk}	1st	1.47	1.47	1.47	1.47	1.47
		2nd	1.462	1.467	1.469	1.469	1.470
	q_t		1.745	1.387	1.47	1.39	1.372
Cd^{2+}	q_{tk}	1st	4.409	4.992	4.999	5	5
		2nd	5	5	5	5	5

	q_t		5.010	5.010	5.010	5.010	5.010

1st: First-order kinetics (Eq. (3)), 2nd: Second-order kinetics (Eq. (4)), Ca-CFA: Calcium-treated coal fly ash

Table 5 Adsorption capacities from experiments and kinetic models for CFA adsorbent

Adsorbate	Adsorption capacity, mg/g		Contact time *(t)*, Minutes				
			10	30	60	240	540
Cu^{2+}	q_{tk}	1st	0.23	0.23	0.23	0.23	0.23
		2nd	0.001	0.027	0.049	0.121	0.167
	q_t		0.122	0.257	0.227	0.215	0.07
Pb^{2+}	q_{tk}	1st	0.74	0.74	0.74	0.74	0.74
		2nd	0.011	0.031	0.060	0.195	0.337
	q_t		0.507	0.787	0.705	0.92	0.77
Cd^{2+}	q_{tk}	1st	0.14	0.14	0.14	0.14	0.14
		2nd	0.012	0.031	0.050	0.093	0.110
	q_t		0.072	0.252	0.085	0.18	0.042

1st: First-order kinetics (Eq. (3)), 2nd: Second-order kinetics (Eq. (4)), CFA: Coal fly ash

Table 6 Qualitative elemental composition of raw CFA and Ca-CFA at t = 30 minutes

Elements	Weight%	
	Raw CFA	Ca-CFA
O	53.46	30.61
Al	15.41	14.22
Si	29.46	29.18
Ca	0.93	8.17
Cu	0.25	5.66
Cd	0.12	9.47
Pb	0.37	2.69

CFA: coal fly ash, Ca-CFA: calcium-treated coal fly ash

List of Figures

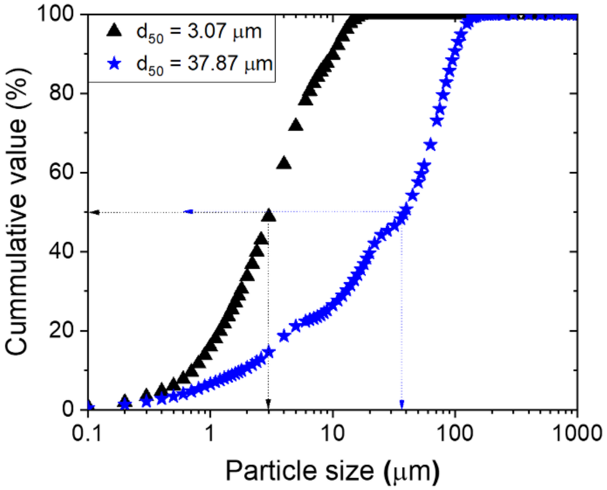

Fig. 1 Particle size distribution of raw coal ash samples

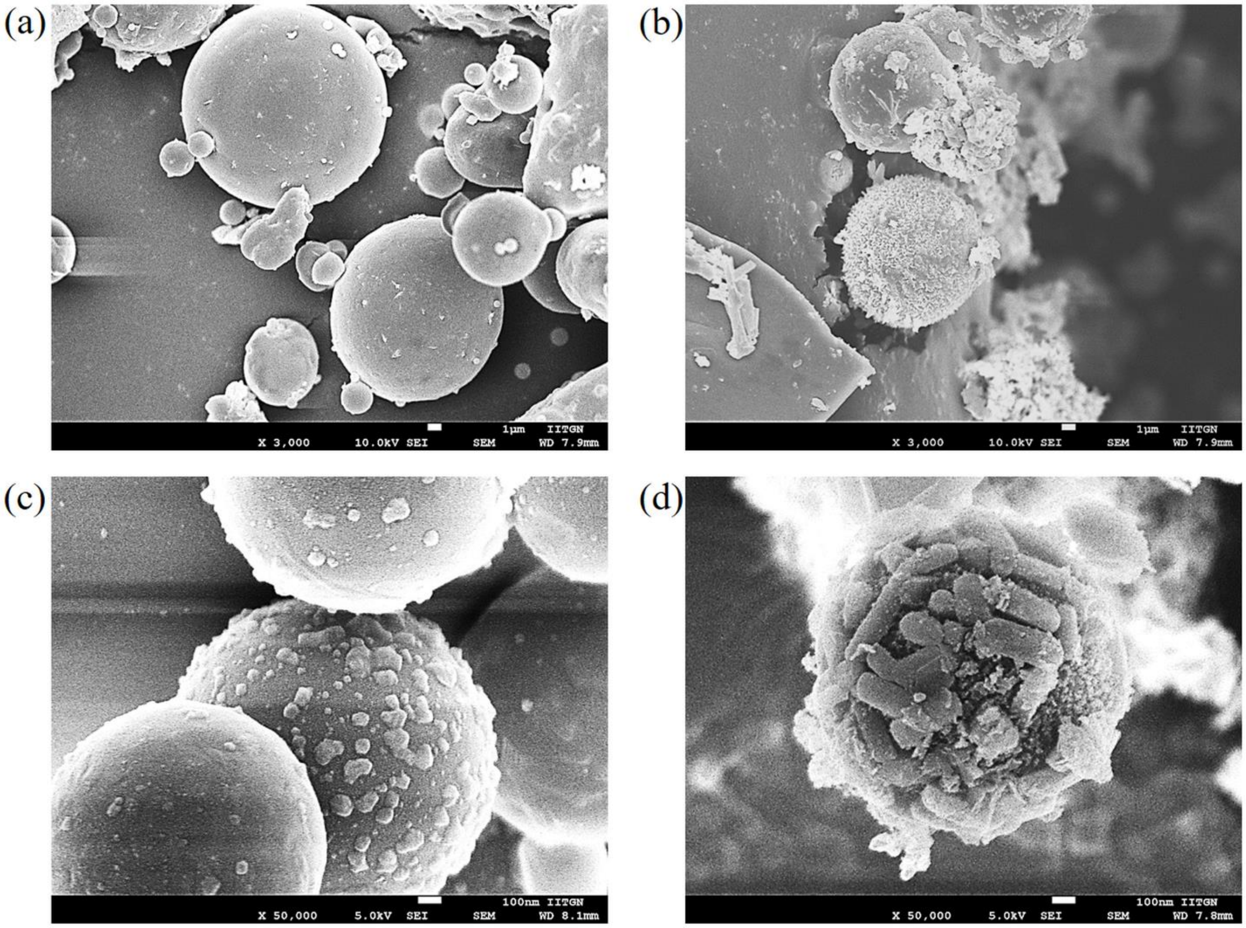

Fig. 2 SEM images of Raw coal ash (a) 3000x (c) 50000x; and Calcium-treated coal ash (b) 3000x (d) 50000x

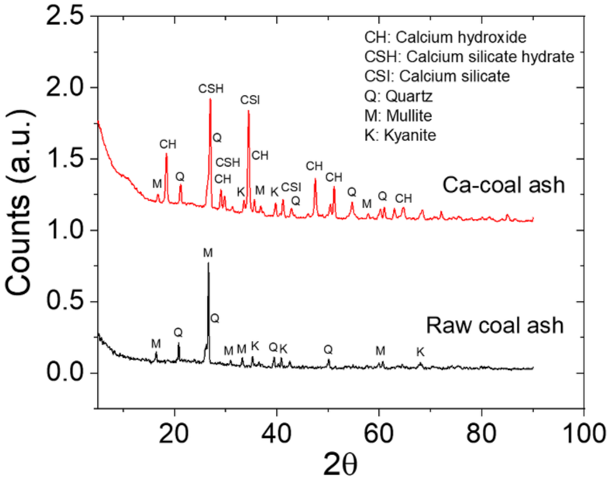

Fig. 3 XRD analysis of raw coal ash and calcium-treated coal ash (Ca-coal ash)

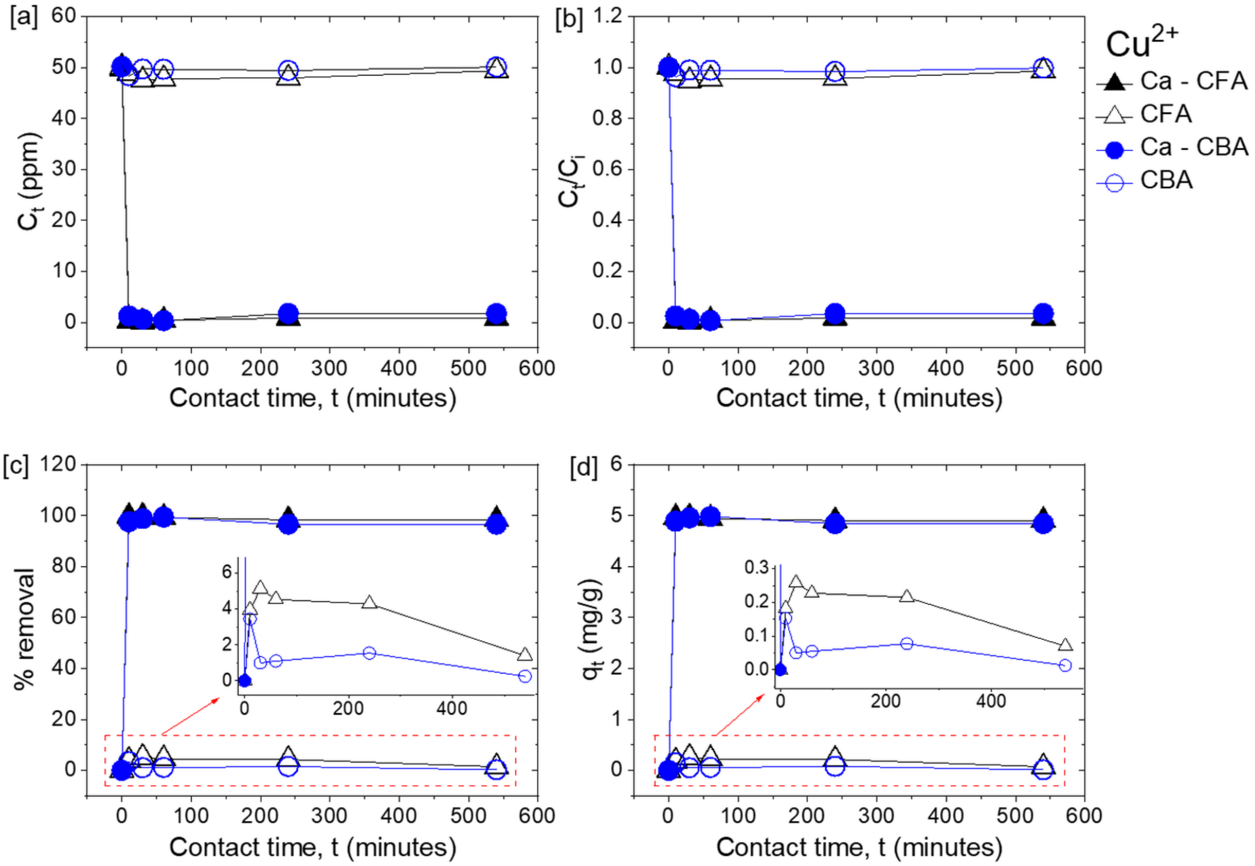

Fig. 4 Adsorption of Cu^{2+} on raw and calcium-treated coal ash (Ca-CFA: Calcium-treated coal fly ash, CFA: Coal fly ash, Ca-CBA: Calcium-treated coal bottom ash, CBA: Coal bottom ash)

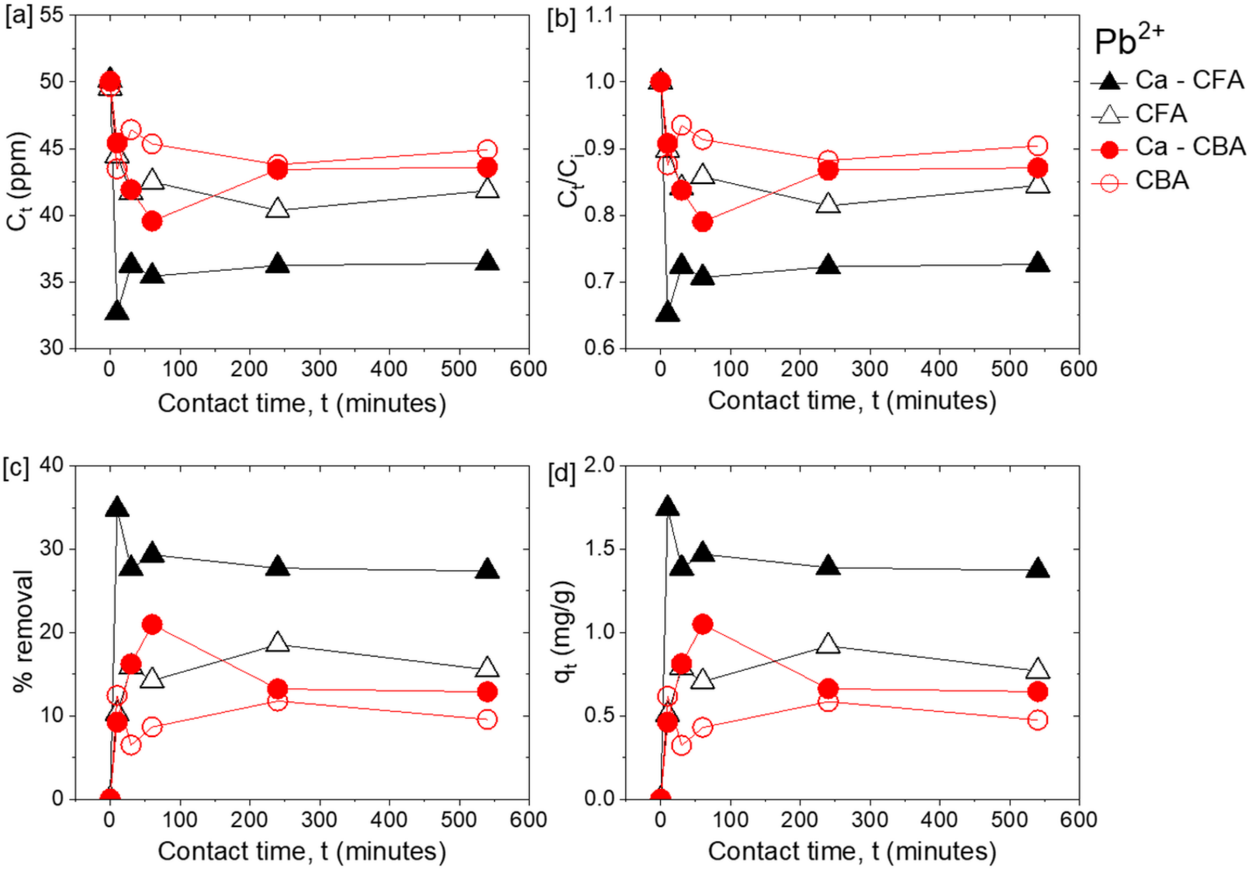

Fig. 5 Adsorption of Pb^{2+} on raw and calcium-treated coal ash (Ca-CFA: Calcium-treated coal fly ash, CFA: Coal fly ash, Ca-CBA: Calcium-treated coal bottom ash, CBA: Coal bottom ash)

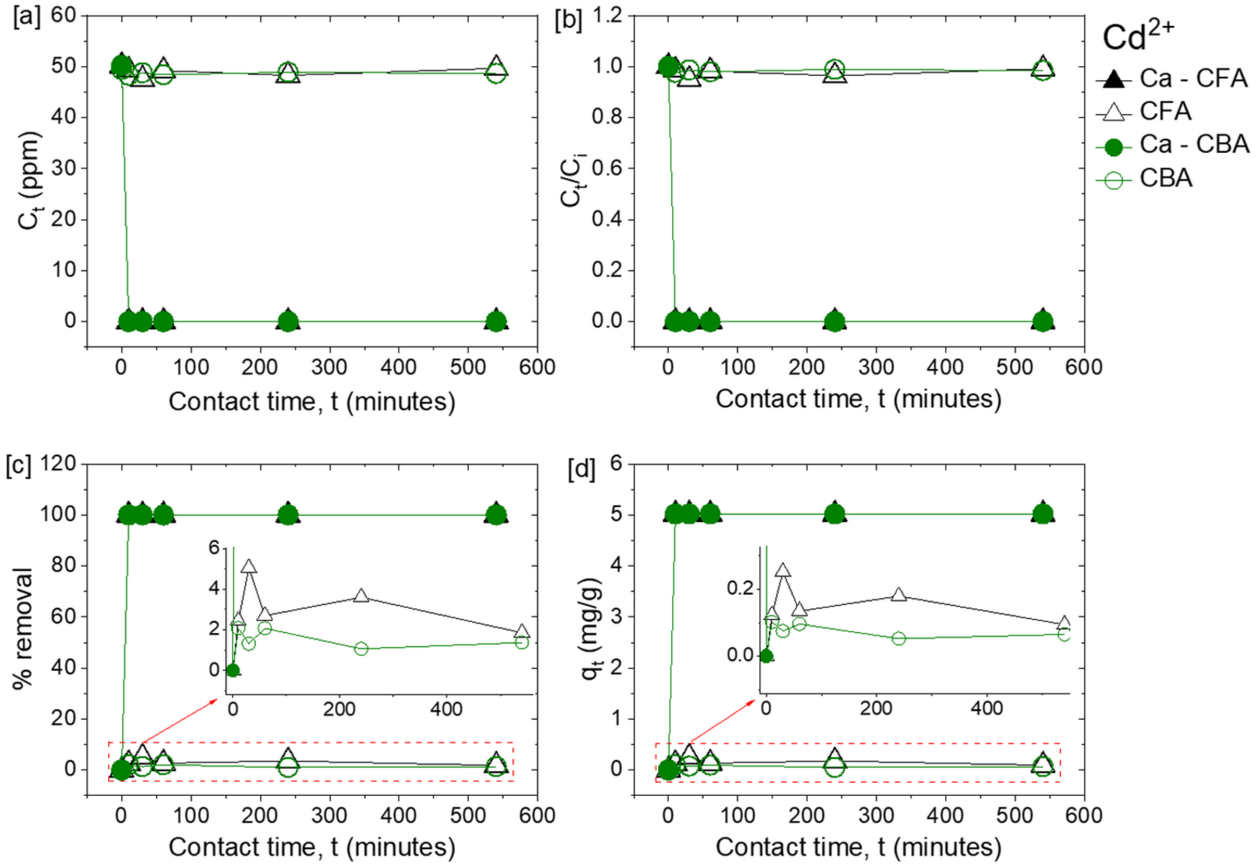

Fig. 6 Adsorption of Cd^{2+} on raw and calcium-treated coal ash (Ca-CFA: Calcium-treated coal fly ash, CFA: Coal fly ash, Ca-CBA: Calcium-treated coal bottom ash, CBA: Coal bottom ash)

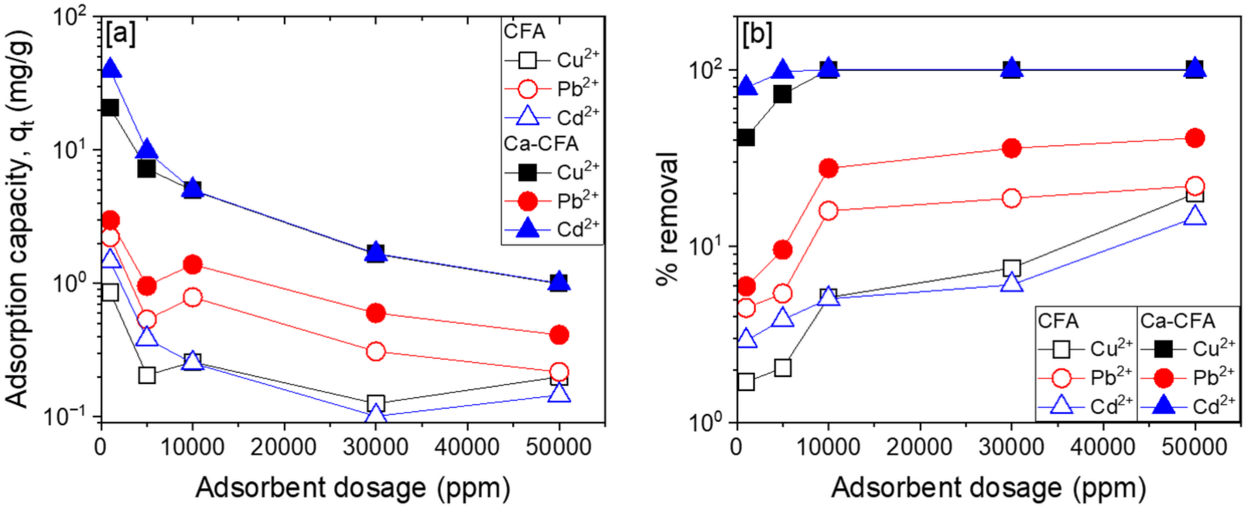

Fig. 7 (a) Adsorption (b) removal efficiency of CFA and Ca-CFA adsorbents varying from 1000-50000 ppm (CFA: Coal fly ash, Ca-CFA: Calcium-treated coal fly ash)

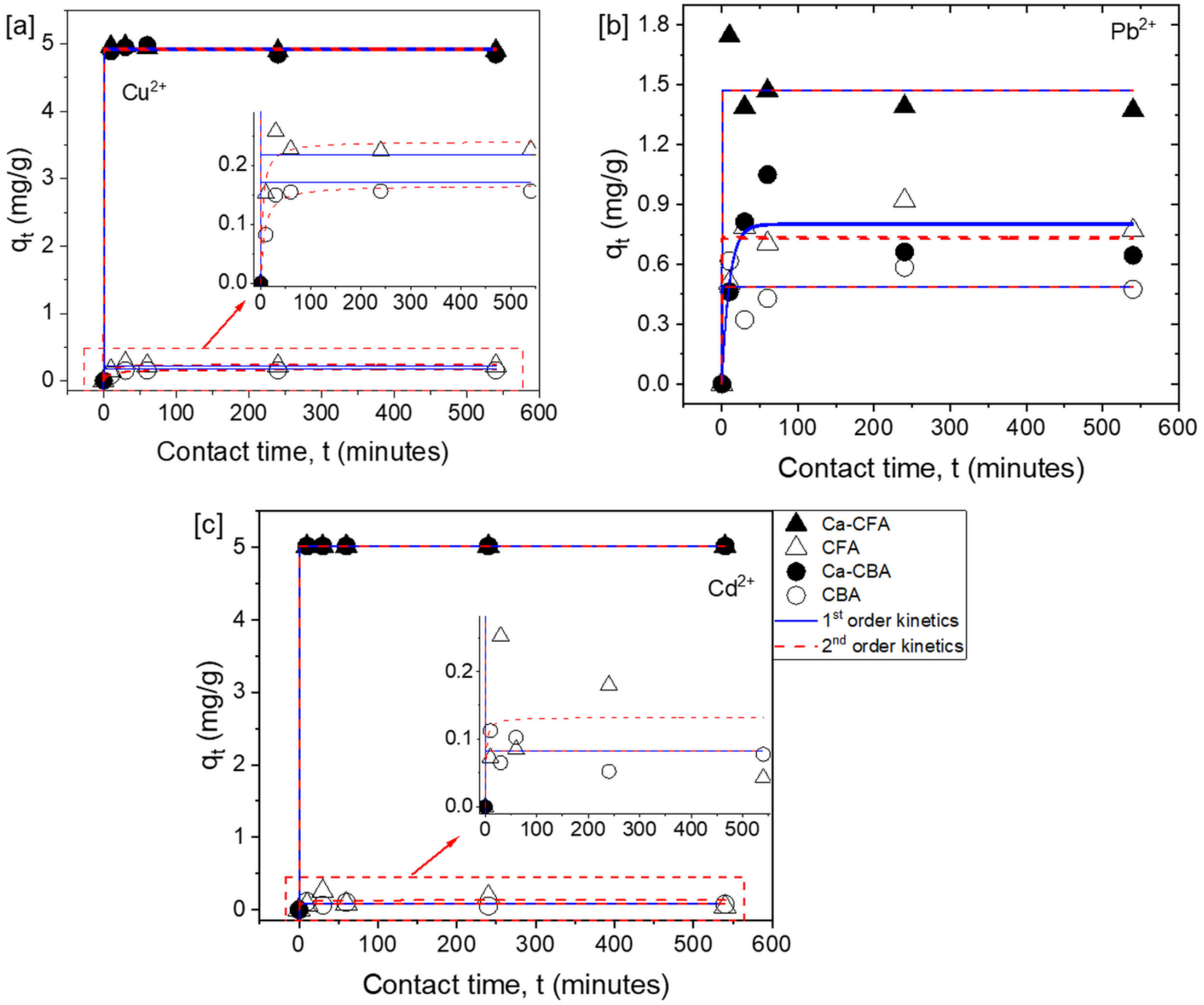

Fig. 8 Adsorption kinetics of Cu^{2+}, Pb^{2+} and Cd^{2+} ions on raw coal ash and calcium-treated coal ash (Ca-CFA: Calcium-treated coal fly ash, CFA: Coal fly ash, Ca-CBA: Calcium-treated coal bottom ash, CBA: Coal bottom ash)

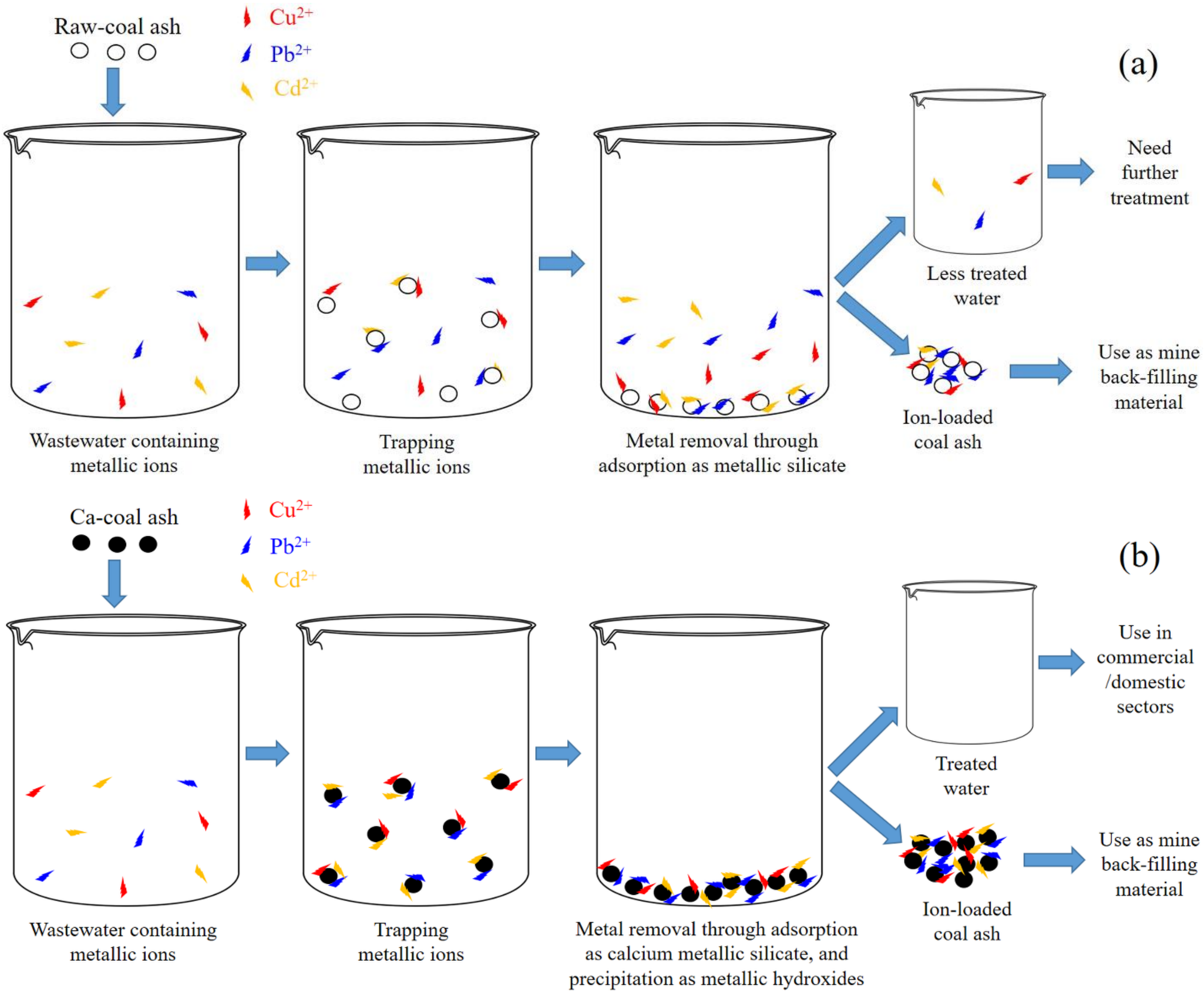

Fig. 9 Metal removal mechanism (a) raw coal ash (b) calcium-treated coal ash (Ca-coal ash)

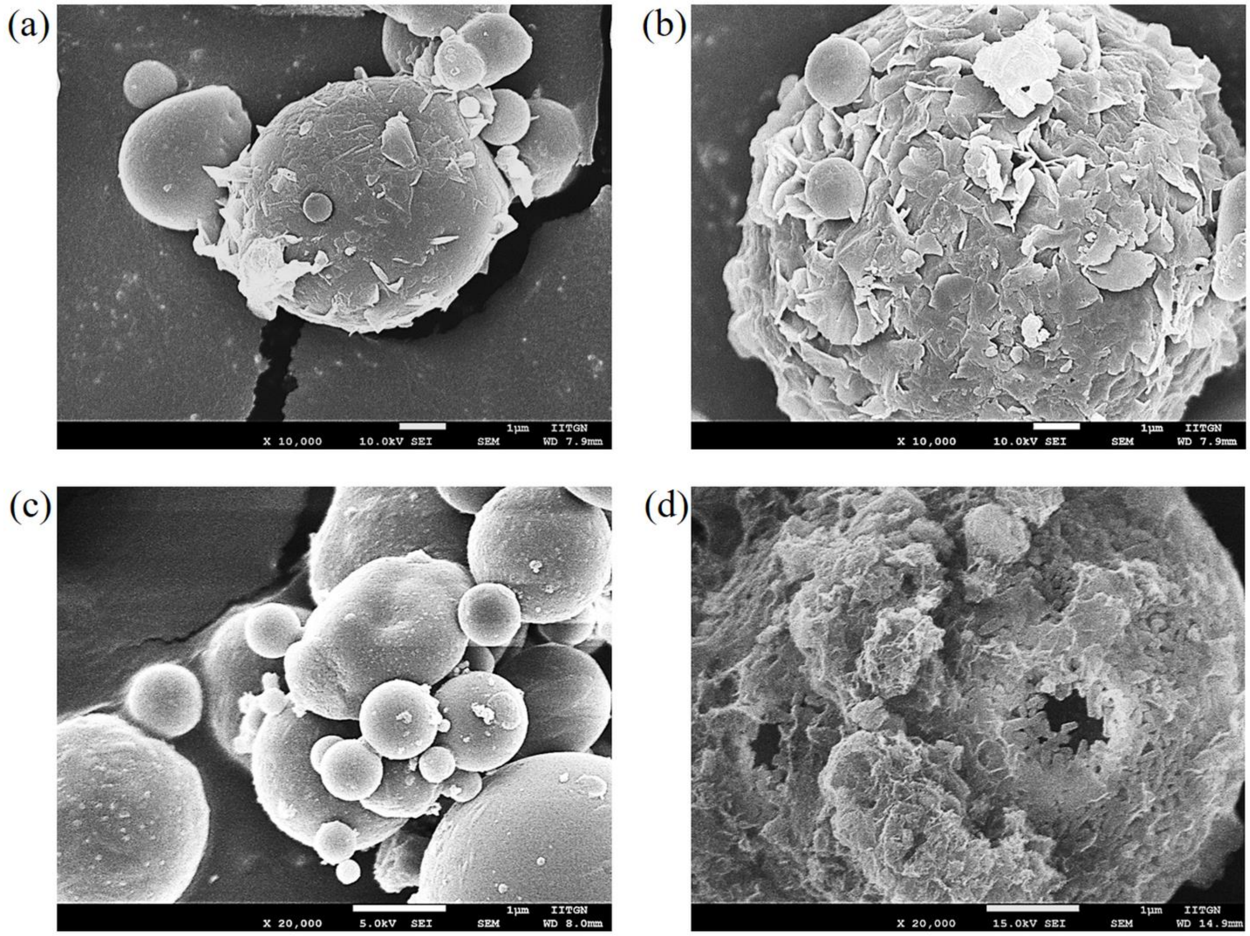

Raw CFA

Ca-CFA

Fig. 10 SEM images of raw CFA (a) 10000x (c) 20000x; and Ca-CFA (b) 10000x (d) 20000x at t = 30 minutes (CFA: coal fly ash, Ca-CFA: calcium-treated coal fly ash)

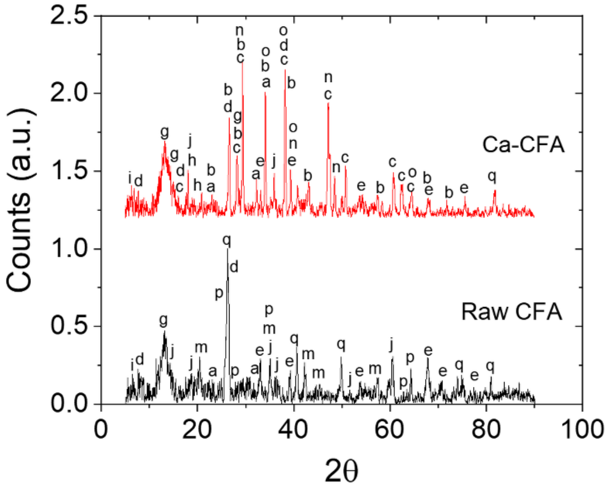

Fig. 11 XRD analysis of raw CFA and Ca-CFA at t = 30 minutes (CFA: coal fly ash, Ca-CFA: calcium-treated coal fly ash, a: Cadmium silicate, b: calcium silicate, c: cadmium hydroxide, d: compound of copper and cadmium, e: Cadmium oxide, g: lead silicate, h: lead hydroxide, i: lead aluminum oxide, j: lead oxide, m: mullite, n: calcium copper silicate, q: quartz, o: copper hydroxide, p: copper oxide)

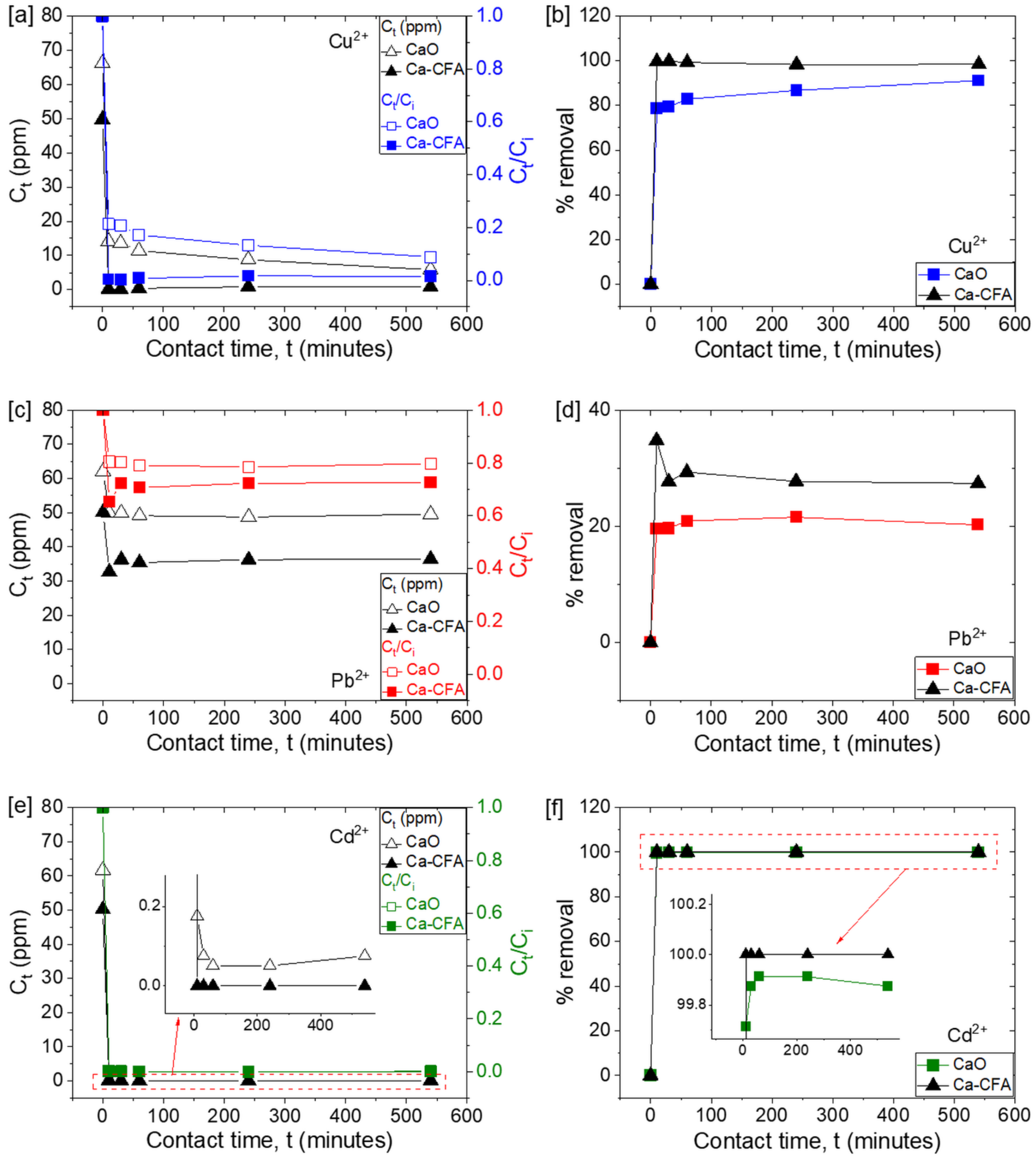

Fig. 12 Adsorption of Cu^{2+}, Pb^{2+}and Cd^{2+} ions on CaO and Ca-CFA (CaO: calcium oxide, Ca-CFA: calcium-treated coal fly ash)

Brief technical biography of the Author

Dr. Vighnesh Prasad is currently working as a Scientist in the Design and Project Engineering Department at CSIR - Institute of Minerals & Materials Technology, Bhubaneswar, India. He received his Bachelor of Engineering (B.E.) degree in Mechanical Engineering Department from OP Jindal University, Raigarh, Chhattisgarh, India. He obtained his Master of Technology (M. Tech.) and Doctor of Philosophy (Ph.D.) degrees in the Department of Materials Engineering and Department of Chemical Engineering, respectively, from the Indian Institute of Technology Gandhinagar, Gujarat, India. He has involved and successfully executed more than 10 research projects funded by government and private organizations. He has published/presented more than 20 research works in reputed journals and conferences. He is the member of various professional bodies, including International Association of Engineer (IAENG), International Society for Research and Development (ISRD), Science and Engineering Institute (SCIEI), International Association of Computer Science and Information Technology (IACSIT).